HIGH TEMPERATURE LOW CYCLE FATIGUE BEHAVIOR OF SUPERALLOY MA 760

A. Hynnä,* V.-T. Kuokkala,* J. Laurila,** and P. Kettunen*

Tampere University of Technology
*Institute of Materials Science
**Research Center for Materials Science
P.O. Box 589, SF-33101 Tampere
Finland

Abstract

The high temperature cyclic behavior of oxide dispersion strengthened superalloy MA 760 was studied at different temperatures and specimen orientations. The cyclic hardening curves at different strain amplitudes were determined at 650°C, 900°C, and 950°C, and the stress-strain response of the material was substantiated by detailed fractographical (SEM) and microstructural (optical microscopy, STEM) observations. During cycling MA 760 did not show marked hardening or softening, and also the final fracture occurred very rapidly with essentially no decrease in the cyclic strength of the material. The "brittle" nature of deformation behavior of MA 760, especially at lower test temperatures, as well as oxidation induced secondary cracking along grain boundaries were clearly revealed by detailed examination of the fracture surfaces. Observation of TEM foils prepared on materials deformed at 650°C, showed evidence of dislocation cutting of γ', but at higher temperatures dislocation climb and bypassing of γ' particles were found to become more prominent features. At all test temperatures, dislocation climb over yttria-particles, as well as the departure side pinning effect of dislocations at non-shearable particles were frequently observed.

Superalloys 1992
Edited by S.D. Antolovich, R.W. Stusrud, R.A. MacKay,
D.L. Anton, T. Khan, R.D. Kissinger, D.L. Klarstrom
The Minerals, Metals & Materials Society, 1992

Introduction

Oxide dispersion strengthened (ODS) superalloys form one of the new material groups developed in search for materials with better properties in extreme operating conditions. They maintain their high strength and good corrosion resistance at higher temperatures than conventional superalloys, and are therefore of great interest, for example, to designers of gas turbine engines (1). ODS superalloys are produced by mechanical alloying process (2) followed by conventional processing and heat treating processes such as: extrusion, hot rolling, recrystallization- and γ'-precipitation heat treatments. The excellent properties of ODS- alloys are due to the very fine dispersion of stable, incoherent oxide particles, formed during the mechanical alloying process. These particles act as barriers to the movement of dislocations (3). ODS Ni-base superalloys can also be strengthened by coherent γ'-precipitates. The γ'-strengthening is acting effectively at lower temperatures than dispersion strengthening, which becomes dominant at temperatures above 1000°C (4). After recrystallization heat treatment, the grain structure of ODS alloys is very coarse and grain aspect ratio is large. Together with highly serrated grain boundaries, the microstructures that develop result in properties that are necessary for high temperature service, where the amount of transverse grain boundaries should be minimized (5).

The creep and fatigue properties of ODS superalloys have been studied intensively during the past few years, but the existing data are still incomplete. This is especially true for MA 760, a modified more corrosion resistant version of the well known MA 6000. In this paper, we report the low cycle fatigue properties of MA 760 at 650°C, 900°C and 950°C together with fractographical (SEM) and microstructural (STEM) observations.

Experimental Procedure

The test material was a mechanically alloyed ODS Ni-base superalloy MA 760 delivered by Wiggin Alloys Ltd. Extruded bars with two different geometries having a small cross section (SCS, 20 mm x 60 mm) and a large cross section (LCS, 32 mm x 95 mm) were delivered. The final heat treatment, given by the supplier, was as follows: 0.5 h at 1120°C, FC at 60°C/min to 600°C + FC. The compositions of the materials in wt-% were the following:

LCS: 19.79%Cr, 5.93%Al, 1.96%Mo, 3.5%W, 1.04%Fe, 0.042%C, 0.14%Zr, 0.286N, 0.003%S, <0.005%P, 0.11%B, 1.03%Y_2O_3, 0.04%Si, 0.60%O

SCS: 19.66%Cr, 5.97%Al, 1.92%Mo, 3.5%W, 1.02%Fe, 0.043%C, 0.14%Zr, 0.284%N, 0.003%S, <0.005%P, 0.11%B, 1.03%Y_2O_3, 0.04%Si, 0.54%O, 0.05%Co, 0.02%Ti

Specimens for the LCF tests were cut from the SCS bar parallel to the extrusion direction (longitudinal direction, L), and from the LCS bar perpendicular to the extrusion direction (long transverse direction, LT). The gauge sections of the samples were surface finished using SiC paper No: 1200. Fatigue tests were conducted using a closed-loop mechanical materials testing machine and a high temperature extensometer attached to the 12.5 mm longitudinal gauge section. Samples were heated using a specially shaped induction coil, which resulted in the maximum measured temperature variation of ±5°C within the gauge length. All tests were performed in air under total strain control using triangular and symmetrical cycles (R_ε = -1), always starting in compression. The strain rate in all tests was 5×10^{-3} s^{-1}.

Results and Discussion

Since the microstructure of virgin MA 760 is not extensively documented, a brief description is given first. The grain structure of MA 760 is very coarse and the grains are elongated in the extrusion direction (Fig. 1a), the GAR being roughly 15. The texture in the extension direction is <110>, in the long transverse direction <111> and in the short transverse direction <112>. The γ'-precipitates are nearly cuboidal with the mean edge length of 0.50 μm. The volume fraction of γ' is close to 50 %. The average dispersoid diameter is 30 nm and the mean spacing between dispersoid particles is about 100 nm. The grain boundaries are mostly low angle boundaries covered with agglomerated γ', as shown in Fig. 1b. Stringers of inclusions extending in the extrusion direction, as well as separate inclusions, possibly nitrides, carbides or oxides, are commonly detected (Fig. 2a). The inclusions often change the chemical composition of the surrounding matrix and thereby the morphology of γ'-precipitates, as illustrated in Fig. 2b. As a result of incomplete secondary recrystallization, small grains are infrequently detected.

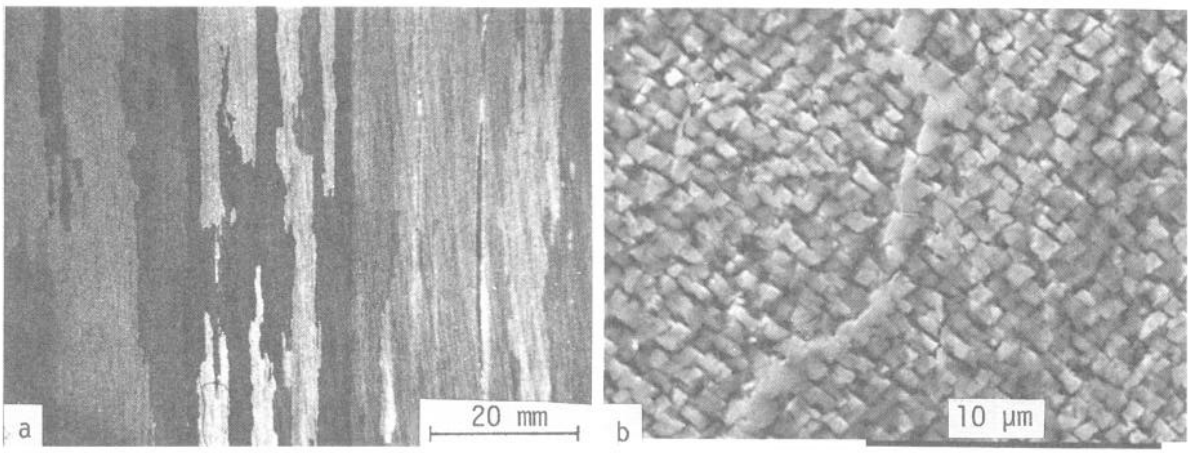

Figure 1 - a) grain structure of MA 760.
b) grain boundary covered with agglomerated γ'.

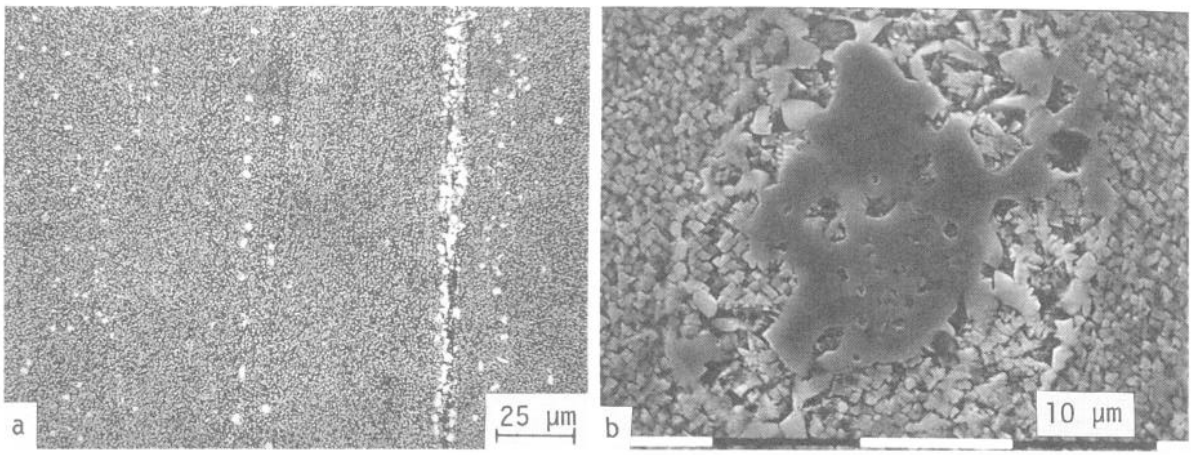

Figure 2 - a) stringers of inclusions extending in the extrusion direction.
b) a typical inclusion with modified γ'-structure around it.

The cyclic hardening curves presented in Fig. 3 show that the stress-strain response of MA 760 at constant amplitude straining does not essentially change during cycling, although a small softening period at the beginning of tests can usually be observed. The tests were conducted under total strain amplitude control but because practically no hardening or softening took place, also the plastic strain amplitudes presented in Table I can be considered to have stayed constant during tests. At the end of the tests, the stress amplitude drops suddenly, especially in tests at 650°C. This indicates that most of the fatigue life is used to initiate crack(s) which

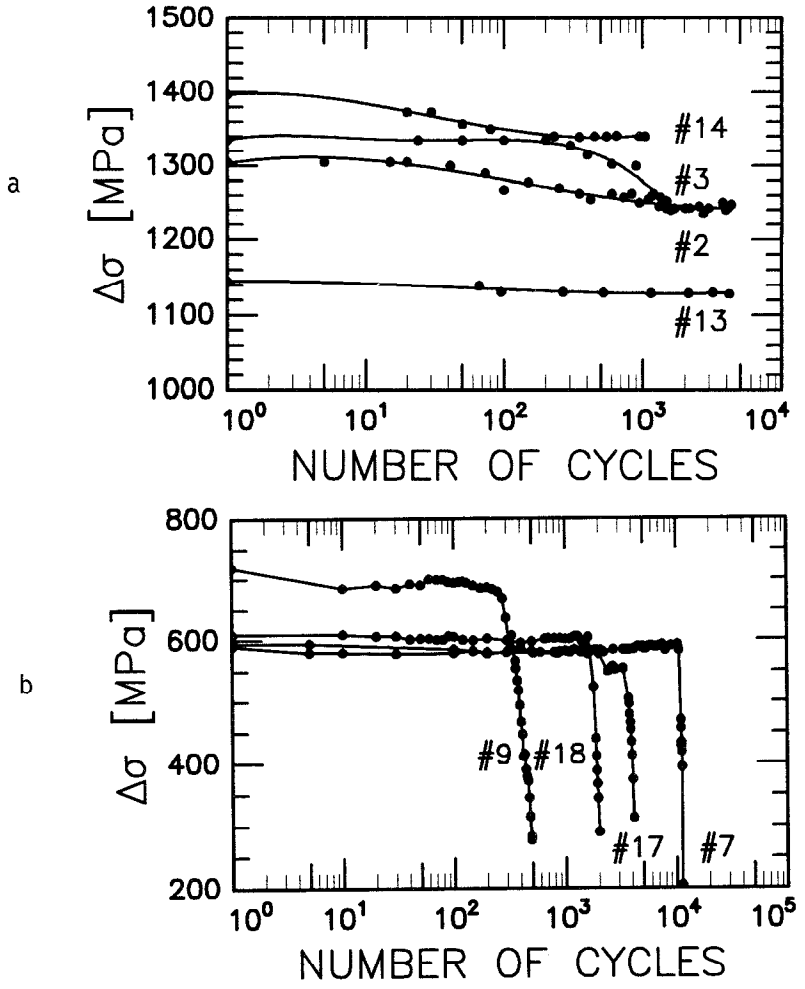

Figure 3 - Cyclic hardening curves: a) T = 650°C, b) T = 900°C and T = 950°C (c.f. Table I for test parameters).

finally propagate very rapidly at the end of the test leading to failure of the specimen. When comparing the fatigue lives of L- and LT-samples, Table I shows that the fatigue lives in the L-direction are longer than in the LT-direction, as expected. When plotting fatigue lives as a function of the plastic strain amplitude, the fatigue lives at 650°C are shorter than those at 900°C or 950°C. For the same amount of plastic deformation, however, much higher stresses are needed at 650°C, which suggests that the crack initiation and early propagation are controlled by local effective stresses at the crack tip rather than by average plastic deformation. This type of behavior is also indicated by the increasing brittleness of the material with decreasing temperature.

Table I Results of low cycle fatigue tests

#	Dir.	T [°C]	$\Delta\varepsilon_t$ [%]	$\Delta\varepsilon_{pl}$ [%]	$\Delta\varepsilon_e$ [%]	$\Delta\sigma$ [MPa]	N_f
1	L	650	0.88	0.01	0.87	1,225	12,480
2	L	650	0.93	0.02	0.91	1,260	4,440
3	L	650	0.98	0.04	0.94	1,330	1,642
4	L	650	1.14	0.05	1.09	1,710	742
5	L	650	1.40	0.23	1.17	1,789	283
6	L	900	0.38	0.02	0.36	412	21,903
7	L	900	0.56	0.02	0.54	588	11,280
8	L	900	0.71	0.17	0.54	628	1,079
9	L	900	0.83	0.20	0.63	700	492
10	L	900	1.34	0.57	0.77	880	198
11	L	900	1.93	1.11	0.82	852	117
12	L	900	2.42	1.50	0.92	948	49
13	LT	650	0.91	0.02	0.89	1,145	5,034
14	LT	650	0.97	0.06	0.91	1,360	1,192
15	LT	650	1.19	0.09	1.10	1,610	636
16	LT	650	1.38	0.12	1.26	1,625	98
17	LT	950	0.55	0.02	0.53	580	4,120
18	LT	950	0.61	0.04	0.57	600	2,021
19	LT	950	0.56	0.15	0.41	580	522
20	LT	950	1.04	0.33	0.71	850	112

= test number, Dir = specimen orientation (L = longitudinal, LT = long transverse), $\Delta\varepsilon_t$ = total strain range, $\Delta\varepsilon_{pl}$ = plastic strain range, $\Delta\varepsilon_e$ = elastic strain range, $\Delta\sigma$ = stress range, N_f = number of cycles to

The studies of fracture surfaces using scanning electron microscope (SEM) revealed that the cracks nucleate at specimen surface in a transgranular mode. On the fracture surface, two distinguishable areas can be observed, small areas with fatigue striations near the initiation point and an almost featureless area associated with the rapid crack growth. The amount of these smooth areas increases with decreasing temperature and increasing stress amplitude.

In the case of the L-samples, transgranular fracture dominates, but at 900°C also intergranular fracture propagating along axially oriented grain boundaries was occasionally observed in the rapid crack growth area. Two typical examples of the fracture surfaces in the L-samples are presented in Fig. 4. In LT-samples, the grains are elongated perpendicular to the loading axis and intergranular fracture (Fig. 5a) is now more common which may explain the reduction in the fatigue lives as compared to those of the L-samples.

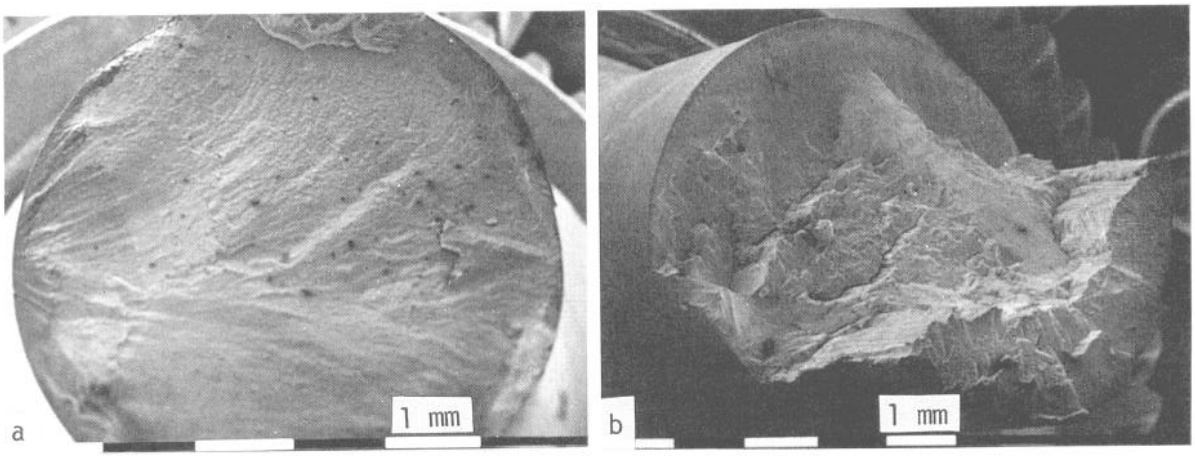

Figure 4 - The fracture surfaces of MA 760. L-samples fatigued at a) $\Delta\varepsilon_t$ = 0.98 %, T = 650°C, b) $\Delta\varepsilon_t$ = 1.93 %, T = 900°C.

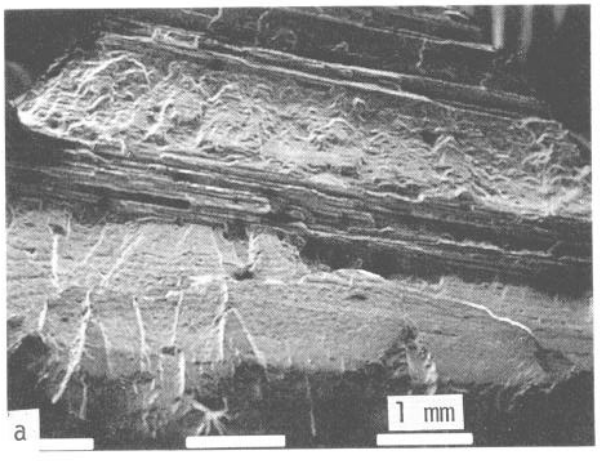

Figure 5 - The fracture surface of a MA 760 LT-sample, fatigued at $\Delta\varepsilon_t$ = 1.04 %, T = 950°C.

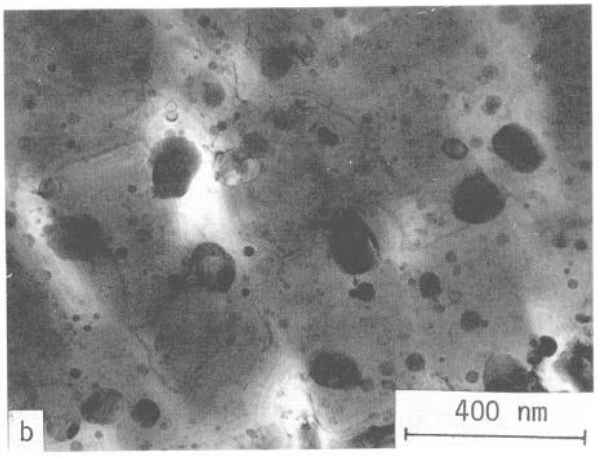

Figure 6 - The microstructure of the as-received MA 760 sample cut perpendicular to the extrusion direction.

The fatigued samples did not show any extensive internal damage, such as voids and non-propagating cracks, apart from localized damage in unrecrystallized regions or at inclusions. These are, however, also non-propagating and do not affect the fracture behaviour. Extensive secondary cracking along grain boundaries across the path of the primary crack was observed in all fatigued samples. It was noticed that cavitation type damage on grain boundaries does not develop and therefore it is likely that the secondary cracking is due to oxidation. At these fairly slow test frequencies, when the crack tip arrives at a grain boundary, there will be time for oxygen diffusion to take place along the grain boundary. On subsequent strain cycles, a secondary crack will nucleate along the boundary and then propagate by a combination of further oxidation and mechanical tearing (6).

Dislocations in the fatigued specimens did not generally form any distinct arrangements normally observed in fatigued metallic materials. The amount of individual dislocations varied as a function of strain amplitude but, e.g., no cell formation was observed. As a function of increasing temperature and fatigue time the γ'-precipitates became bigger and more rounded, which is usually referred to as the Ostwald ripening. Especially at 650°C, but also occasionally at higher temperatures, paired dislocations, which are indications of γ'-cutting, were observed (8). At 900°C and 950°C, dislocations were commonly surrounding the γ'-precipitates pointing to the bypassing mechanism of γ'. Also the lack of hardening, and the saturation of the cyclic stress amplitude observed point to a dislocation bypassing mechanism (9).

Dislocation climb over yttria particles was detected at all test temperatures. Dislocations were often pinned to the departure sides of Y_2O_3 particles and curved in areas between them. The departure side pinning is explained by the attractive interaction between the dislocations and the interface of incoherent particles and it seems to be a common strengthening mechanism in ODS superalloys (7). Fig. 6 shows the microstructure of undeformed MA 760 and Figs 7a and 7b typical microstructures after cyclic straining at 650°C and 900°C.

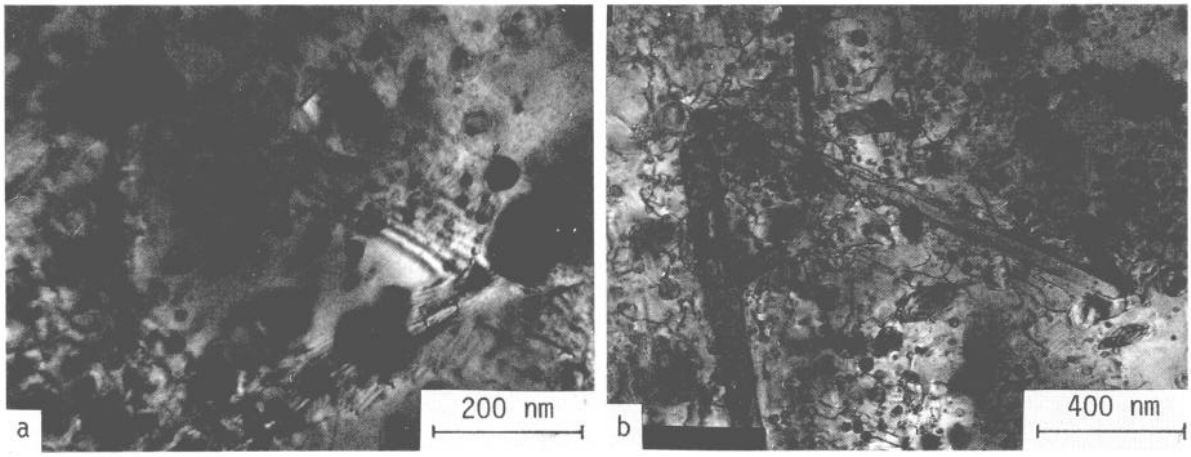

Figure 7 - Microstructures of fatigued MA 760. TEM samples cut parallel to the fatigue specimen: a) LT-sample, $\Delta\varepsilon_t$ = 0.91 %, T = 650°C, b) L-sample, $\Delta\varepsilon_t$ = 0.56 %, T = 900°C.

Conclusions

1. The fatigue failure of MA 760 takes place without noticeable change in the stress-strain response of the material. The dislocations detected around γ'-precipitates tend to indicate that dislocation bypassing deformation mechanism is operative.

2. At 650°C, the deformation capability of MA 760 is extremely limited and the fracture surfaces contain only small areas of actual fatigue striations near the crack initiation site. Most of the failure surface areas have a "brittle" appearance.

3. Oxidation induced secondary cracking along grain boundaries perpendicular to the main crack growth direction were observed in all test conditions.

References

1. G.W. Meethan, "Superalloys in Gas Turbine Engines", Met. and Mat. Tech., 14, (1982), 387-392.

2. J.S. Benjamin, "Mechanical Alloying",Sci. Am., 5, (1978), 40-48.

3. Y. Kaieda, "Trends in Development of Oxide-Dispersion-Strengthened Superalloys", Trans. Nat. Res. Inst. Metals, 28, (3) (1986), 18-24.

4. M.J. Fleetwood, "Mechanical Alloying - The Development of Strong Alloys", Mat. Sci. Tech., 2, (1986), 1176-1182.

5. H. Zeizinger and E. Arzt, "The Role of Grain Boundaries in High Temperature Creep Fracture of an Oxide Dispersion Strengthened Superalloy", Z. Metallkde, 79, (1988), 774-781.

6. A. Tekin and J. W. Martin, "Fatigue Crack Growth Behaviour of MA 6000", Mat. Sci. Eng., 96, (1987), 41-49.

7. E. Arzt and S.D. Wilkinson, "Threshold Stresses for Dislocation Climb over Hard Particles: The Effect of an Attractive Interaction", Acta Met., 34, (1986), 1893-1898.

8. E. Nembach and G. Neite, "Precipitation Hardening of Superalloys by Ordered '-particles", Prog. Mat. Sci., 29, (1985), 177-319.

9. J. Bressers and E. Arzt, "High Temperature Low Cycle Fatigue of Inconel MA 6000", High Temperature Alloys for Gas Turbines and Other Applications 1986, ed. W. Betz et al. (Liége, Belgium, C.R.M., 1986), 1067-1080.